DOI: 10.1002/ejic.200700251

# Liquid Crystal Imidazolium Salts: Towards Materials for Catalysis and Molecular Electronics

Jean-Moïse Suisse,[a] Laurent Douce,*[a] Stéphane Bellemin-Laponnaz,[b]
Aline Maisse-François,[b] Richard Welter,[b] Yasuo Miyake,[c,d] and Yo Shimizu[c]

**Keywords:** Liquid crystals / Imidazolium ions / Pd–carbenes / Homogenous catalysis / Conducting materials

1,3-Bis(4-alkyloxyphenyl)-3*H*-imidazol-1-ium trifluoromethanesulfonates, alkyl = $CH_3(CH_2)_{n-1}$, $n$ = 8, 10, 12, 14 and 16, can be derived from the analogous 4-alkyloxyphenylamines. These imidazolium salts exhibit a lamellar liquid-crystal mesophase between 99 °C and 191 °C. The smectic-A phase was fully characterised by polarising optical microscopy, differential scanning calorimetry and X-ray diffraction. We report also the synthesis, lamellar crystal structure and catalytic activity of the $Pd^{II}$ complex of the (deprotonated) carbene form of one of these salts. In addition, we measured the charged carrier mobilities in the mesophase.

## Introduction

Extensive studies of ionic liquids have revealed their many useful properties such as their extremely low volatility, high thermal stability, nonflammability, high chemical stability, high ionic conductivity and wide electrochemical window.[1] Such salts are extremely versatile in that changes in both the cation and its counteranion can be used to tune their properties, which for imidazolium salts in particular includes their mesomorphism.[2] The merging of imidazolium ionic liquids and liquid-crystal chemistry has indeed begun to lead to a new range of materials[1d,3] with applications in, for example, dye-sensitised solar cells,[4] electron transport systems[3b] and nanoparticle electrosynthesis.[5] Variation of the imidazolium N-substituents is a facile means of creating this range. Of additional interest is the fact that the salts can be readily deprotonated to give, formally, N-heterocyclic carbenes that are excellent ligands for transition-metal-based catalysts.[6]

Herein, we wish to report the synthesis of imidazolium liquid crystals as well as the synthesis and catalytic activity of a $Pd^{II}$ carbene complex derived from a mesomorphic imidazolium species.

## Results and Discussion

### Synthesis

Compounds **1a**–**e** were obtained − as described previously for **1c**[7] − in a two-step procedure from aniline derivatives (Scheme 1). Condensation of the aniline derivatives with glyoxal followed by treatment with chloromethyl pivalate in the presence of 1 equiv. of silver triflate gave corresponding imidazolium salts **1a**–**e** in good yields, all of which were unequivocally characterised by $^1H$ and $^{13}C\{^1H\}$ NMR, UV and FTIR spectroscopy, as well as elemental analysis.

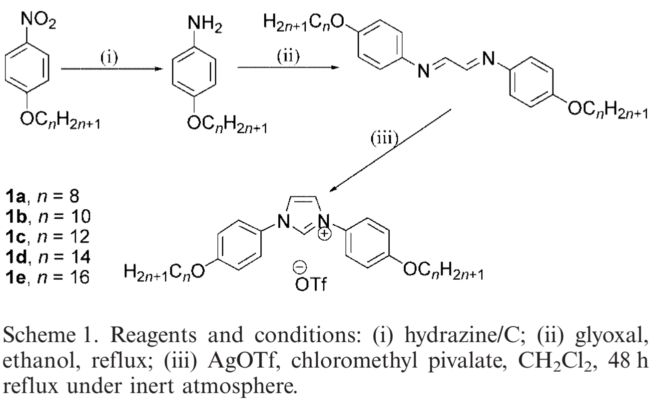

Scheme 1. Reagents and conditions: (i) hydrazine/C; (ii) glyoxal, ethanol, reflux; (iii) AgOTf, chloromethyl pivalate, $CH_2Cl_2$, 48 h reflux under inert atmosphere.

---

[a] Institut de Physique et Chimie des Matériaux de Strasbourg, Groupe des Matériaux Organiques, UMR 7504, CNRS-Université Louis Pasteur,
B. P. 43, 23 rue du Loess, 67034 Strasbourg Cedex 2, France
Fax: +33-388-107-246
E-mail: laurent.douce@ipcms.u-strasbg.fr
[b] Institut de Chimie, Université Louis Pasteur, UMR CNRS 7177-LC003, Laboratoire DECOMET,
4 rue Blaise Pascal, 67000 Strasbourg, France
[c] Synthetic Nano-Function Materials Group, Nanotechnology Research Institute, National Institute of Advanced Industrial Science and Technology (AIST), Kansai centre,
Midorigaoka 1-8-31, Ikeda, Osaka, 563-8577 Japan
[d] Graduate School of Engineering, Osaka Electro-Communication University,
Hatscho, Neyagawa, Osaka, 572-8530 Japan

### Mesomorphic Properties

The mesomorphic behaviour and phase-transition temperatures were characterised by polarising optical microscopy (POM), differential scanning calorimetry (DSC) and X-ray diffractometry (XRD). The phase-transition temperatures and their corresponding enthalpy changes for compounds **1a**–**e** are compiled in Table 1, whereas typical results are displayed in Figure 1.

Table 1. Phase-transition temperatures (°C) and corresponding enthalpies $\Delta H$ (J/mmol) were determined from the first heating; abbreviations: Cr = crystalline phase, LC = smectic-A phase, I = isotropic phase.

| Compound | $T$ [°C] Cr → LC | $T$ [°C] LC → I |
|---|---|---|
| **1a** | 120.0 (48.51) | 126.0 (3.09) |
| **1b** | 116.0 (57.55) | 158.0 (3.78) |
| **1c** | 117.0 (80.03) | 175.7 (4.60) |
| **1d** | 118.3 (71.91) | 183.9 (3.87) |
| **1e** | 113.4 (108.44) | 191.1 (3.46) |

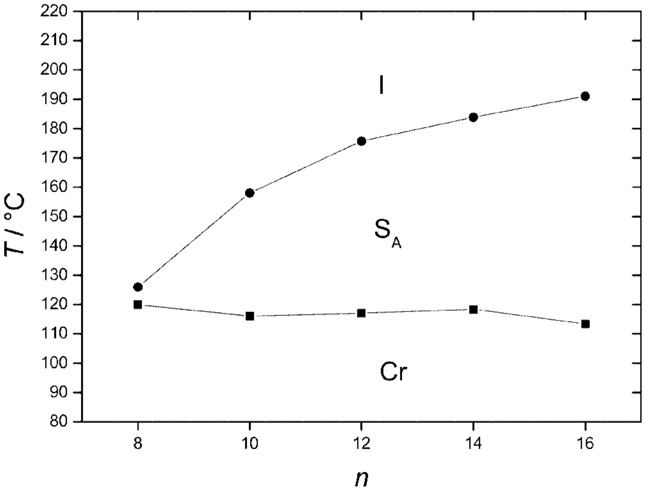

Figure 1. Phase diagram of compounds **1a**–**e** (I: isotropic liquid; $S_A$: smectic-A phase; Cr: crystalline phase).

The high stability of the compounds was demonstrated by the absence of significant perturbation of the DSC patterns following several heating–cooling cycles. The peak occurring at the lowest temperature (see Table 1 and Figure 1) corresponds to the melting of the crystal into a smectic-A phase. Determined by random motions of the paraffinic moiety, this peak involves an important enthalpy change that increases linearly with the number of carbon atoms of the tails (see Figure 2, ■).

The corresponding slope $(7.2 \pm 0.9)$ KJ/mol gives a value of the melting enthalpy of the methylene groups of $(258 \pm 32)$ J/g, comparable to that found for the complete melting of linear paraffins (289 J/g)[8] or for the transition of crystalline mesogens into a smectic phase (272[9a] and 238[9b] J/g).

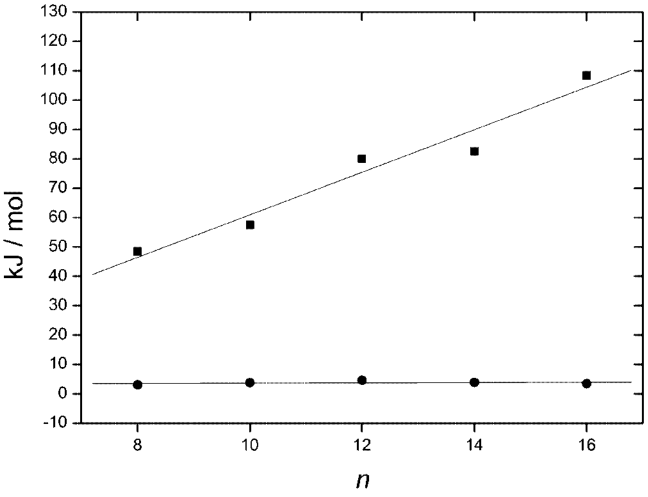

Figure 2. Phase transition enthalpies as a function of the number of carbon atoms in the alkyl chains; ■, Cr–$S_A$; ●, $S_A$–I.

The peak corresponding to the transition from the smectic-A phase to the isotropic liquid, related to the disordering of the aromatic cores of the molecules, involves an enthalpy that is independent of the length of the molecules, as expected and observed (see Figure 2, ●).

The liquid-crystalline phase was also confirmed by optical microscopy. The optical textures observed during slow cooling from isotropic melt showed the emergence of a smectic-A phase (see Figure 3a–b, initial appearance of rods turning into wide, fan-like, focal-conic textures).

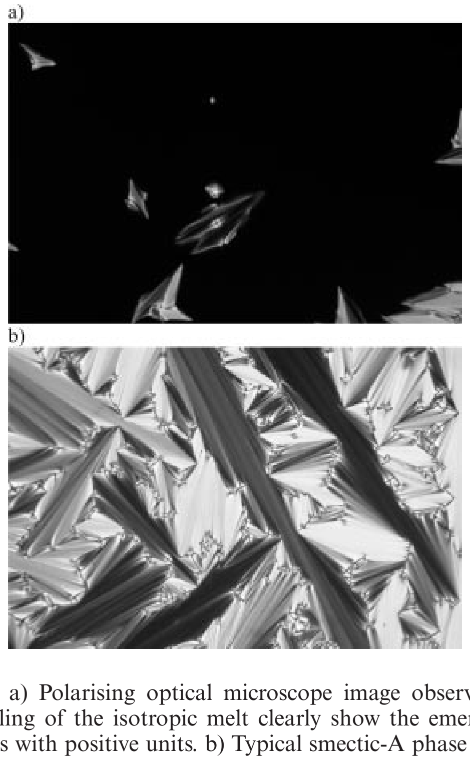

Figure 3. a) Polarising optical microscope image observed upon slow cooling of the isotropic melt clearly show the emergence of Batônnets with positive units. b) Typical smectic-A phase obtained from **1c** between 117 and 175 °C.

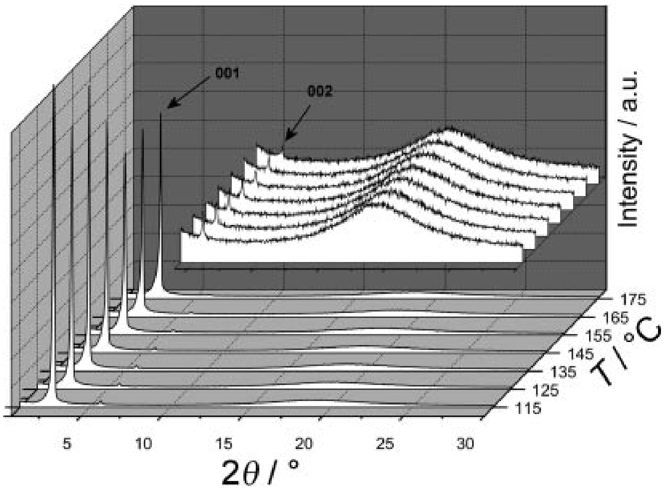

Figure 4. X-ray diffraction pattern of the smectic-A phase of **1c** at different temperatures. For clarity the intensities of the peak 002 and the broad band at Bragg angles $2\theta \geq 5°$ have been magnified.

The smectic-A arrangement is definitively established by the presence of two sharp, equidistant reflections (ratio 1:2) in the small angle region, related to smectic layering, and a broad band in the wide angle region, related both to the disordered conformation of the alkyl chains and the liquid-like lateral correlations of the aromatic core within the layers (Figure 4).

This mesophase was also evident in the XRD patterns, allowing determination of the *d*-spacing values for the smectic-A phase as shown in Figure 5. It is important to note that the smectic period increases in a linear manner with the molecular size.

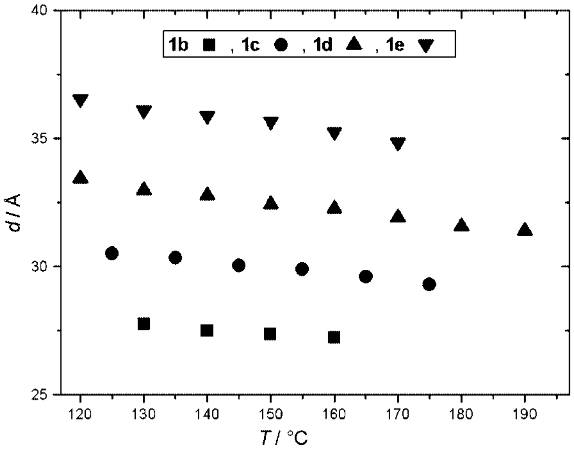

Figure 5. Variation of the smectic period of **1a**–**e** in the smectic-A state as a function of the number of carbon atoms in the alkyl chains and at different temperatures.

## Palladium(II) Carbene Complex

Transformation of imidazolium salts **1a**–**e** into N-heterocyclic carbene complexes was of interest in regard to possible applications in catalysis. Thus, palladium(II) complex **2** was obtain by deprotonation of imidazolium **1b** in the presence of the palladium salt precursor $Pd(OAc)_2$, KO*t*Bu (1 equiv.) and NaI (4 equiv.) (Scheme 2).[10] The formulation of complex **2** was confirmed by elemental analysis. The presence of a carbene centre was established by the observation of a signal at $\delta$ = 167.0 ppm in the $^{13}C$ NMR spectra, which was assigned to the 2C-imidazol-2-ylidene carbon nucleus, and by the absence of the resonance for the 2H-imidazolium proton in the $^{1}H$ NMR spectra. The details of the molecular structure of palladium carbene complex **2** in the solid state were established by a single-crystal X-ray diffraction study. The molecular unit present in the crystal is shown in Figure 6.

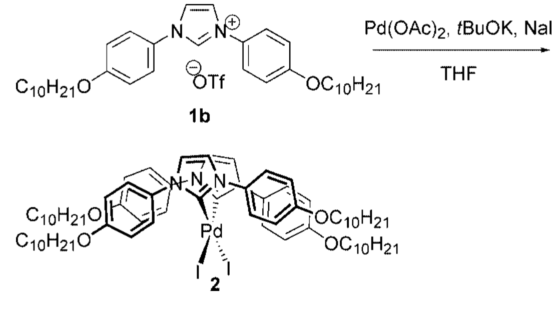

Scheme 2. Conditions: 12 h at room temp.

As shown in Figure 6, the $Pd^{II}$ centre is bound to two carbene ligands with a *cis* coordination geometry. The metal has a square-planar coordination sphere [C1–Pd–C36, 89.8(1)°; I–Pd–I, 92.42(4)°], with the heterocyclic rings near-perpendicular to the coordination plane and to one another.

The Pd–I [2.6788(3) and 2.6620(8) Å] and Pd–C bond lengths [2.009(3) and 2.000(4) Å] are similar to those in related complexes.[11] The *cis* geometry is probably favoured by a combination of steric and electronic factors involving the Pd centre as well as π–π interactions between the phenyl groups of the two heterocyclic ligands[12] [centroid distances of 3.54(2) and 3.66(2) Å for C20–C25/C55–C60 and C4–C9/C39–C44, respectively, labelled *x* in Figure 7). This in-

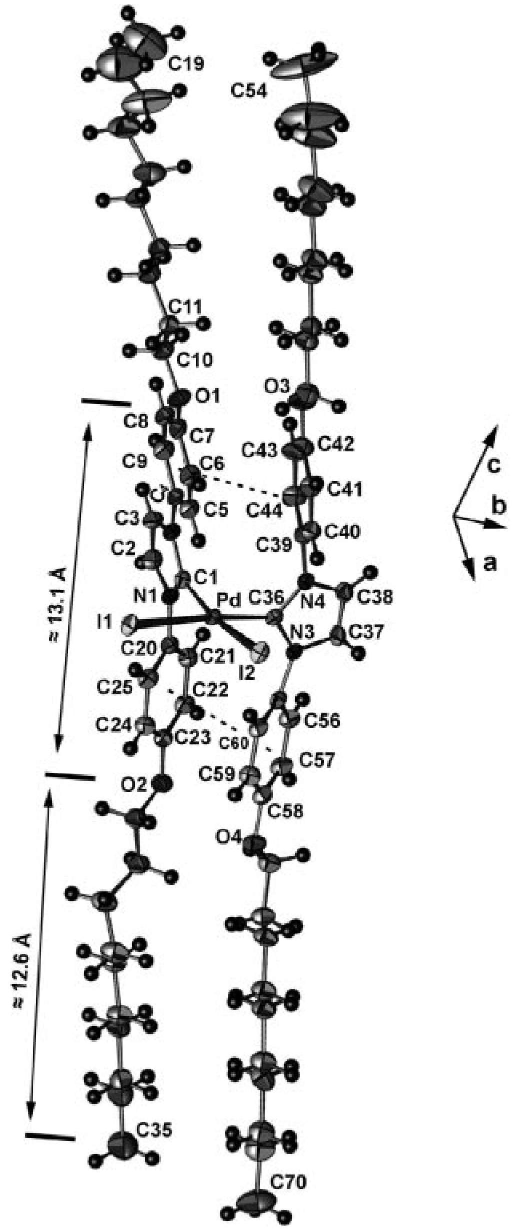

Figure 6. ORTEP view of the crystal structure asymmetric unit of complex **2** with partial labelling scheme. Thermal ellipsoids enclose 50% of the electronic density. Dashed lines indicate the intramolecular phenyl–phenyl π–π interactions.

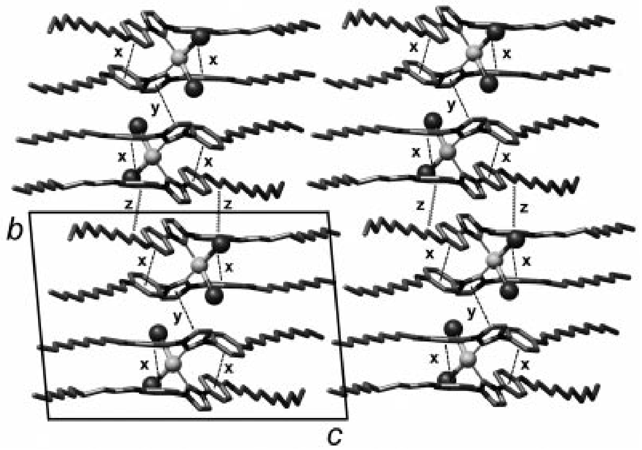

Figure 7. Solid-state packing diagram of complex **2** in projection on the (*b*,*c*) plane. The π–π and CH–π interactions are labelled with *x* (intramolecular π–π), *y* (intermolecular π–π) and *z* (intermolecular CH–π).

teraction may also account for the orientation of the phenyl rings towards the heterocyclic carbene. The length of the rigid part of the molecule is around 13.1 Å, whereas the length of the alkoxy chain is around 12.6 Å (see Figure 6).

No classical hydrogen bonds were detected in this crystal structure. Nevertheless, careful analysis of the intermolecular approaches provided evidence for three nonclassical hydrogen bonds involving the iodine and carbon atoms of both the phenyl and heterocyclic rings.

These presumably weak hydrogen contacts[13] are listed in Table 2. The crystal packing can be interpreted in terms of a combination of CH–π and π–π interactions.[13] The intermolecular π–π interactions (labelled *y* in Figure 7) occurring between the heterocycles force them to be strictly parallel. Another π–π weak interaction is detected between both C36–N3–C37–C38–N4 rings of two adjacent molecules along the *b* axis [with a centroid distance of 3.90(2) Å].

Table 2. Weak hydrogen interactions with iodine atoms.

| C–H···I | $d_{\text{C–H}}$ [Å] | $d_{\text{H–I}}$ [Å] | $d_{\text{C–I}}$ [Å] | C–H–I angle [°] |
|---|---|---|---|---|
| C25–H25···I1 | 0.95 | 2.99 | 3.8954 | 159 |
| C37–H37···I2 | 0.95 | 3.02 | 3.8384 | 146 |
| C60–H60···I2 | 0.95 | 2.93 | 3.8223 | 156 |

Finally, the CH–π interactions (C10–H10B···phenyl group and C11–H11A···phenyl group; labelled *z* in Figure 7) probably explain the form of the array along the crystallographic *b* axis.

## Catalysis Behaviour

Cross-coupling reactions represent an extremely versatile tool in organic synthesis. In order to explore the potential of our imidazolium salts as a source of N-heterocyclic carbene ligands for palladium-catalysed cross-coupling reactions, we decided to investigate the Suzuki–Miyaura reaction with imidazolium **1b** (Scheme 3).[14] Optimised conditions were used for the Suzuki–Miyaura cross-coupling: Pd(OAc)$_2$/imidazolium salt (2 equiv.), $Cs_2CO_3$ as base and dioxane as solvent (80 °C).[15]

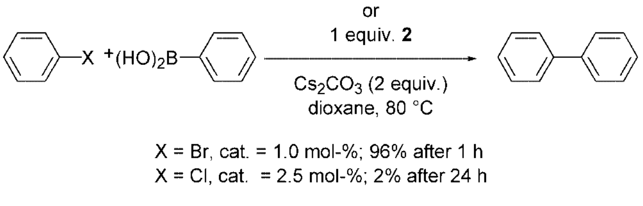

Scheme 3. Suzuki–Miyaura reaction.

The coupling of bromobenzene and phenylboronic acid proceeds quite rapidly in high yields with a catalyst loading of 1.0 mol-% (96% GC yield after 1 h). However, we were not able to observe catalysis for the coupling of chlorobenzene and phenylboronic acid even with a higher catalyst loading (2.5 mol-%). Similar results were obtained by using palladium complex **2**. It is known that steric factors dictate the catalytic activity since bulky N-substituents in the imidazolium salt are required to get good catalytic activity. The presence of the alkoxy chain in the *para* position of the *N*-aryl imidazolylidene does not change the efficiency of the ligand in the cross-coupling. Therefore, imidazolium **1b** with two $C_{10}H_{21}$ alkyl tails acts as a ligand with the same reactivity as 1,3-bis(4-methylphenyl)imidazolylidene.[15]

### Mobility of Charged Carriers in the Mesophase

The carrier mobility measurements were carried out for the smectic-A phase of **1b** by using the time-of-flight (TOF) technique (Figure 8). As preliminary data, the mobility for the positive electrode illumination was estimated to be in the order of $10^{-4}$ cm$^2$/V s, which is comparable to those of nematic liquid crystals ($10^{-4}$–$10^{-6}$ cm$^2$/V s)[16] and the lower ordered smectic liquid crystals.[17–19]

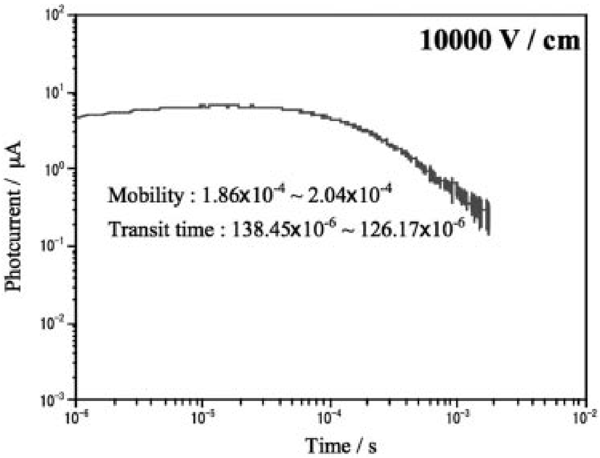

Figure 8. Typical decay curve of the transient photocurrent observed in the TOF measurements (bias: 10000 V/cm). The mesophase is smectic-A phase (131 °C) and the compound was not uniformly aligned in the cell gap (2.56 µm-thick).

This mobility is in a region where both electronic and ionic transports of charged carriers should be considered. It might indicate that both ionic transport and electronic hopping could be realised in the liquid-crystalline phase of this compound, though the reality of carriers is unknown for this mobility.

## Conclusions

We report the full characterisation of new mesomorphic compounds based on an imidazolium unit with different alkyls tails. We investigated the ability of the conjugate base of the cation to form carbene complexes with palladium(II). Preliminary measurements of the charged carrier mobility in the mesophase suggest electronic as well as ionic transports. To evaluate the influence of the supramolecular architecture on catalysis or palladium-catalysed reactions, we are now investigating the ability of this palladium(II) carbene complex to be dissolved in an ionic liquid crystal.

## Experimental Section

**Synthesis:** All commercially available chemicals were used without further purification. Dichloromethane (DCM) was carefully dried and distilled prior to use. Full details of the salt and Pd$^{II}$ complex syntheses will be given elsewhere, though all bisimines were obtained as indicated in Figure 1.[7] The new compounds were characterised by NMR spectroscopy and elemental analyses. With appropriate variations of the alkoxyphenyl diimine starting material (Figure 1), all imidazolium triflates were prepared by the method described below for octyloxy species **1a**.

**1,3-Bis(4-octyloxyphenyl)-3*H*-imidazol-1-ium Trifluoromethanesulfonate (1a):** To a mixture of the octyloxy bisimine (0.521 g, 1.12 mmol) and AgOTf (0.317 g, 1.23 mmol) was added dry $CH_2Cl_2$ (25 mL) and then chloromethyl pivalate (305 µL, 2.103 mmol). The mixture was stirred in the dark at 50 °C, under an argon atmosphere, for 20 h. The solution was cooled to room temp., the mixture was filtered through Celite, the solvent was evaporated and the crude product was purified by silica gel column chromatography ($CH_2Cl_2$ then $CH_2Cl_2$/MeOH, 95:5). The compound was subsequently crystallised from dichloromethane by the addition of hexane. The imidazolium triflate deposited as colourless crystals. (0.413 g, 59%). $^1$H NMR (300 MHz, $CDCl_3$, 20 °C): $\delta$ = 9.64 (t, $^4J$ = 1.23 Hz, N–CH–N imidazolium), 7.67 (d, $^4J$ = 1.60 Hz, 2 H, N–CH–CH–N imidazolium), 7.65 (m, $^3J$ = 9.0 Hz, 2 H, aromatic, AA′ system), 7.04 (m, $^3J$ = 9.0 Hz, 2 H, aromatic, BB′ system), 3.90 (t, $^3J$ = 6.60 Hz, 2 H, $CH_2$–O), 1.80 (m, 2 H, $CH_2$–$CH_2$–O), 1.44 (m, 2 H, $CH_2$–$CH_2$–$CH_2$–O), 1.32 (br. s, 16 H, aliphatic), 0.90 (t, $^3J$ = 7.0 Hz, 3 H, $CH_3$) ppm. $^{13}$C NMR (75 MHz, $CDCl_3$, 20 °C): $\delta$ = 14.04 (–$CH_3$), 22.61, 25.91, 29.03 29.17, 29.29, 31.76, 68.59 (O–$CH_2$), 115.90, 120.63 (q, $J$ = 320 Hz, $CF_3$) 121.98, 123.39, 124.82, 126.88, 132.35, 160.58 ppm. IR (KBr pellet): $\tilde{\nu}$ = 3141 and 3102 (C–H aromatic), 2918 and 2852 (C–H aliphatic), 1555 and 1513 (C=N imidazolium), 1266 ($OTf^-$) cm$^{-1}$. $\lambda$ ($\varepsilon$) = 277 (16375) nm. $C_{32}H_{45}F_3N_2O_5S$ (626.77): calcd. C 61.32, H 7.24, N 4.47; found C 61.36, H 7.25, N 4.44.

**1,3-Bis(4-decyloxyphenyl)-3*H*-imidazol-1-ium Trifluoromethanesulfonate (1b):** Yield crystalline solid (4.39 g; 82%) $^1$H NMR (300 MHz, $CDCl_3$, 20 °C): $\delta$ = 9.64 (t, $^4J$ = 1.56 Hz, N–CH–N imidazolium), 7.66 (d, $^4J$ = 1.74 Hz, 2 H, N–CH–CH–N imidazolium), 7.65 (m, $^3J$ = 6.78 Hz, 2 H, aromatic, AA′ system), 7.03 (m, $^3J$ = 6.78 Hz, 2 H, aromatic, BB′ system), 3.97 (t, $^3J$ = 6.36 Hz, 2 H, $CH_2$–O), 1.80 (m, 2 H, $CH_2$–$CH_2$–O), 1.43 (m, 2 H, $CH_2$–$CH_2$–$CH_2$–O), 1.29 (br. s, 24 H, aliphatic), 0.89 (t, $^3J$ = 6.97 Hz, 3 H, $CH_3$) ppm. $^{13}$C NMR (75 MHz, $CDCl_3$, 20 °C): $\delta$ = 14.05 (–$CH_3$), 22.62, 22.85, 25.90, 26.11, 29.04, 29.27, 29.35, 29.52, 31.84, 68.55 (O–$CH_2$), 115.84, 120.65 (q, $J$ = 320 Hz, $CF_3$), 122.09, 123.30, 126.87, 132.02, 160.49 ppm. IR (KBr pellet): $\tilde{\nu}$ = 3143 and 3102 (C–H aromatic), 2917 and 2851 (C–H aliphatic), 1555 and 1513 (C=N imidazolium), 1265 ($OTf^-$) cm$^{-1}$. $\lambda$ ($\varepsilon$) = 277 (21977) nm. $C_{36}H_{53}F_3N_2O_5S$ (682.88): calcd. C 63.32, H 7.82, N 4.10, S 4.70; found C 63.10, H 7.97, N 3.89, S 4.75.

**1,3-Bis(4-dodecyloxyphenyl)-3*H*-imidazol-1-ium Trifluoromethanesulfonate (1c):** Yield crystalline solid (0.600 g, 61%). $^1$H NMR

(300 MHz, $CDCl_3$, 20 °C): $\delta$ = 9.59 (t, $^4J$ = 1.65 Hz, N–CH–N imidazolium), 7.67 (d, $^4J$ = 1.60 Hz, 2 H, N–CH–CH–N imidazolium), 7.64 (m, $^3J$ = 9.0 Hz, 2 H, aromatic, AA′ system), 7.01 (m, $^3J$ = 9.0 Hz, 2 H, aromatic, BB′ system), 3.95 (t, $^3J$ = 6.6 Hz, 2 H, $CH_2$–O), 1.79 (m, 2 H, $CH_2$–$CH_2$–O), 1.43 (m, 2 H, $CH_2$–$CH_2$–$CH_2$–O), 1.28 (br. s, 32 H, aliphatic), 0.89 (t, $^3J$ = 7.0 Hz, 3 H, $CH_3$) ppm. $^{13}C$ NMR (75 MHz, $CDCl_3$, 20 °C): $\delta$ = 14.10 (–$CH_3$), 22.69, 25.97, 29.10, 29.36, 29.41, 29.60, 29.63, 29.65, 29.68, 31.92, 68.65 (O–$CH_2$), 120.68 (q, $J$ = 320 Hz, $CF_3$), 122.02, 123.44, 126.86, 132.40, 160.64 ppm. IR (KBr pellet): ṽ = 3141 and 3102 (C–H aromatic), 2917 and 2852 (C–H aliphatic), 1555 and 1513 (C=N imidazolium), 1266 ($OTf^-$) $cm^{-1}$. $\lambda$ ($\varepsilon$) = 276 (18400) nm. $C_{40}H_{61}F_3N_2O_5S$ (738.98): calcd. C 65.01, H 8.32, N 3.79, S 4.34; found C 64.78, H 8.58, N 4.25, S 3.56.

**1,3-Bis(4-tetradecyloxyphenyl)-3*H*-imidazol-1-ium Trifluoromethanesulfonate (1d):** Yield crystalline solid (0.479 g; 58%). $^1H$ NMR (300 MHz, $CDCl_3$, 20 °C): $\delta$ = 9.64 (t, $^4J$ = 1.74 Hz, N–CH–N imidazolium), 7.66 (d, $^4J$ = 1.70 Hz, 2 H, N–CH–CH–N imidazolium), 7.64 (m, $^3J$ = 7.02 Hz, 2 H, aromatic, AA′ system), 7.03 (m, $^3J$ = 6.99 Hz, 2 H, aromatic, BB′ system), 3.97 (t, $^3J$ = 6.57 Hz, 2 H, $CH_2$–O), 1.80 (m, 2 H, $CH_2$–$CH_2$–O), 1.43 (m, 2 H, $CH_2$–$CH_2$–$CH_2$–O), 1.27 (br. s, 40 H, aliphatic), 0.88 (t, $^3J$ = 7.02 Hz, 3 H, $CH_3$) ppm. IR (KBr pellet): ṽ = 3143 and 3101 (C–H aromatic), 2917 and 2850 (C–H aliphatic), 1555 and 1513 (C=N imidazolium), 1265 ($OTf^-$) $cm^{-1}$. $\lambda$ ($\varepsilon$) = 277 (27047) nm. $C_{44}H_{69}F_3N_2O_5S$ (795.09): calcd. C 66.47, H 8.75, N 3.52, S 4.03; found C 66.35, H 8.77, N 3.48, S 4.17.

**1,3-Bis(4-hexadecyloxyphenyl)-3*H*-imidazol-1-ium Trifluoromethanesulfonate (1e):** Yield crystalline solid (0.376 g; 34%). $^1H$ NMR (300 MHz, $CDCl_3$, 20 °C): $\delta$ = 9.72 (t, $^4J$ = 1.53 Hz, N–CH–N imidazolium), 7.65 (d, $^4J$ = 1.53 Hz, 2 H, N–CH–CH–N imidazolium), 7.67 (m, $^3J$ = 7.03 Hz, 2 H, aromatic, AA′ system), 7.03 (m, $^3J$ = 7.0 Hz, 2 H, aromatic, BB′ system), 3.99 (t, $^3J$ = 6.57 Hz, 2 H, $CH_2$–O), 1.81 (m, 2 H, $CH_2$–$CH_2$–O), 1.41 (m, 2 H, $CH_2$–$CH_2$–$CH_2$–O), 1.27 (br. s, 40 H, aliphatic), 0.89 (t, $^3J$ = 7.0 Hz, 3 H, $CH_3$) ppm. $^{13}C$ NMR (75 MHz, $CDCl_3$, 20 °C): $\delta$ = 14.06 (–$CH_3$), 22.64, 25.91, 29.02, 29.31 29.53, 29.60, 29.57, 29.66, 31.87, 68.65 (O–$CH_2$), 116.05, 121.82, 123, 126.78, 132.26, 160.80 ppm. IR (KBr pellet): ṽ = 3141 and 3102 (C–H aromatic), 2918 and 2852 (C–H aliphatic), 1555 and 1513 (C=N imidazolium), 1266 ($OTf^-$) $cm^{-1}$. $\lambda$ ($\varepsilon$) = 277 (18438) nm. $C_{48}H_{77}F_3N_2O_5S$ (851.20): calcd. C 67.73, H 9.12, N 3.29; found: C 67.75, H 8.98, N 3.39.

**Palladium–Carbene Complex 2:** Compound **1b** (250.0 mg, 0.367 mmol), $Pd(OAc)_2$ (41.2 mg, 0.183 mmol) and NaI (55.0 mg, 0.367 mmol) were suspended in THF (15 mL). *t*BuOK (41.1 mg, 0.367 mmol) was added to the suspension under an atmosphere of nitrogen. The resulting solution was stirred for 1.5 d at 40 °C. After evaporation of the solvent, the residue was extracted with dichloromethane/water. After drying the DCM layer over $Na_2SO_4$ and evaporating it to dryness, the orange solid was purified by flash column chromatography ($SiO_2$, $CH_2Cl_2$/pentane). Yield: 116 mg, 44%. $^1H$ NMR (300 MHz, $CDCl_3$): $\delta$ = 7.51 (d, $J$ = 8.9 Hz, 4 H), 6.96 (s, 2 H), 6.75 (d, $J$ = 8.9 Hz, 4 H), 4.05 (t, $J$ = 6.6 Hz, 4 H), 1.86 (m, 4 H), 1.53–1.26 (m, 28 H), 0.89 (t, $J$ = 6.7 Hz, 6 H) ppm. $^{13}C$ NMR (75 MHz, $CDCl_3$): $\delta$ = 167.0 ($C_{\text{carbene}}$), 158.5 ($C_q$), 133.0 ($C_q$), 127.8 (CH), 123.8 (CH), 114.5 (CH), 68.2, 31.9, 29.7, 29.6, 29.5, 29.4, 29.3, 26.2, 22.7, 14.1 ($CH_3$) ppm. $C_{71}H_{105}I_2N_3O_4Pd$ (1424.84): calcd. C 59.0, H 7.3, N 3.9; found C 58.95, H 7.45, N 3.80.

**General Procedure for the Suzuki-Type Coupling Reactions:** Palladium acetate (1–2.5 mol-%), imidazolium salt (2–5 mol-%), $Cs_2CO_3$ (652 mg, 2 mmol) and phenylboronic acid (183 mg, 1.5 mmol) were added to a small Schlenk tube under an atmosphere of nitrogen. Dioxane (3 mL) and the aryl halide (1 mmol) were then added, and the mixture was heated in an oil bath at 80 °C. At the conclusion of the reaction, the reaction mixture was cooled and analysed by GC–MS.

**Carrier Mobility Measurements:** The charge carrier mobility in the mesophase was measured by TOF (time-of-flight) measurement apparatus equipped with a polarising microscope and a hot stage. The light source was a pulsed nitrogen gas laser (Nippon Laser, $\lambda$ = 337 nm, 0.8 ns). The cells consisting of ITO- and $TiO_2$-coated glasses for an asymmetric structure of sandwich-type cells were mounted on the hot stage and electric bias was applied by a stabilised DC power supply. The resulting photocurrent was detected with a digital oscilloscope with a homemade preamplifier.

**X-ray Crystallography:** The selected crystal was mounted on a Nonius Kappa-CCD area detector diffractometer (Mo-$K_\alpha$, $\lambda$ = 0.71073 Å). The complete conditions of data collection (Denzo software) and structure refinements are given below. The cell parameters were determined from reflections taken from one set of ten frames (1.0° steps in phi angle), each at 20 s exposure. The structures were solved by direct methods (SHELXS97) and refined against $F^2$ using the SHELXL97 software. All non-hydrogen atoms were refined anisotropically. Hydrogen atoms were generated according to stereochemistry and refined by using a riding model in SHELXL97.[20] CCDC-628899 contains the supplementary crystallographic data for this paper. These data can be obtained free of charge from The Cambridge Crystallographic Data Centre via www.ccdc.cam.ac.uk/data_request/cif. Colourless single crystal; crystal dimension: $0.10 \times 0.08 \times 0.05$ $mm^3$. $C_{70}H_{104}I_2N_4O_4Pd$, $M$ = 1425.77 g/mol; Triclinic; space group $P\bar{1}$; $a$ = 10.7060(1) Å; $b$ = 15.8080(2) Å; $c$ = 21.6950(3) Å; $Z$ = 2; $D_{\text{calcd.}}$ = 1.354 g/cm; $\mu$ (*Mo-$K_a$*) = 1.195 $mm^{-1}$; a total of 20389 reflections; 1.34 ° $< \theta <$ 30.06°, 1842 independent reflections with 12376 having $I > 2\sigma(I)$; 730 parameters; Final results: $R_1$ = 0.0460; $wR_2$ = 0.1287, *Goof* = 0.996, maximum residual electronic density = 1.887 e/$Å^3$.

## Acknowledgments

We are especially grateful to D. Guillon and J. Harrowfield for the critical evaluation of this manuscript, we also thank A. De Cian for the X-ray diffraction studies. This work was supported by the Institut for Physics and Chemistry of Materials Strasbourg (I. P. C. M. S), the Institut of Chemistry and Louis Pasteur University.

---

[1] a) P. Wasserscheid, T. Welton in *Ionic Liquids in Synthesis*, Wiley-VCH, Weinheim, **2003**; b) J. Dupont, R. F. de Souza, P. A. Suarez, *Z. Chem. Rev.* **2002**, *102*, 3667–3692; c) C. E. Song, *Chem. Commun.* **2004**, 1033–1043; d) H. Ohno, *Electrochemical Aspects of Ionic Liquids*, Wiley-Interscience, **2005**; e) J. M. Crosthwaite, S. N. V. K. Aki, E. J. Maginn, J. F. Brennecke, *J. Phys. Chem. B* **2004**, *108*, 5113–5119; f) M. Yoshizawa, W. Xu, C. A. Angell, *J. Am. Chem. Soc.* **2003**, *125*, 15411–15419; g) A. J. Fry, *J. Electroanal. Chem.* **2003**, *546*, 35–39.

[2] a) R. B. Rogers, K. R. Seddon (Eds.), *ACS Symposium Series No. 901: Ionic Liquids IIIA: Fundamental, Progress, Challenges and Opportunities*, American Chemical Society, Washington DC, **2005**; b) R. B. Rogers, K. R. Seddon (Eds.), *ACS Symposium Series No. 902:Ionic Liquids IIIB: Fundamental, Progress, Challenges and Opportunities*, American Chemical Society, Washington DC, **2005**.

[3] a) K. Binnemans, *Chem. Rev.* **2005**, *105*, 4148–4204; b) M. Yoshio, T. Mukai, H. Ohno, T. Kato, *J. Am. Chem. Soc.* **2004**, *126*, 994–995; c) C. J. Bowlas, D. W. Bruce, K. R. Seddon,

*Chem. Commun.* **1996**, 1625–1626; d) C. M. Gordon, J. D. Holbrey, A. R. Kennedy, K. R. Seddon, *J. Mater. Chem.* **1998**, *8*, 2627–2636; e) A. E. Bradley, C. Hardacre, J. D. Holbrey, S. Johnston, S. E. J. McMath, M. Nieuwenhuyzen, *Chem. Mater.* **2002**, *14*, 629–635; f) J. De Roche, C. M. Gordon, C. T. Imrie, M. D. Ingram, A. R. Ingram, A. R. Kennedy, F. LoCelso, A. Triolo, *Chem. Mater.* **2003**, *15*, 2003; g) K.-M. Lee, Y.-T. Lee, J. B. Lin, *J. Mater. Chem.* **2003**, *13*, 1079–1084; h) J. Y. Z. Chiou, J. N. Chen, J. S. Lei, I. J. B. Lin, *J. Mater. Chem.* **2006**, *16*, 2972–2977; i) W. Dobbs, L. Douce, L. Allouche, A. Louati, F. Malbocs, R. Welter, *New J. Chem.* **2006**, *30*, 528–532.

[4] a) J. Motoyanagi, T. Fukushima, T. Aida, *Chem. Commun.* **2005**, 101–103; b) S. Kumar, S. Kumar Pal, *Tetrahedron Lett.* **2005**, *46*, 2607–2610.

[5] a) A. Taubert, P. Steiner, A. Mantion, *J. Phys. Chem. B* **2005**, *109*, 15542–15547; b) A. Taubert, *Acta Chim. Slov.* **2005**, *52*, 183–186; c) A. Taubert, *Angew. Chem. Int. Ed.* **2004**, *43*, 5380–5382; d) W. Dobbs, J.-M. Suisse, L. Douce, R. Welter, *Angew. Chem. Int. Ed.* **2006**, *45*, 4179–4182.

[6] a) W. A. Herrmann, *Angew. Chem. Int. Ed.* **2002, 41**, *8*, 1290–1309; b) D. Bourissou, O. Guerret, F. Gabbaï, G. Bertrand, *Chem. Rev.* **2000**, *100*, 39–92; c) W. A. Herrmann, C. Köcher, *Angew. Chem. Int. Ed. Engl.* **1997**, *36*, 2162–2187; d) V. César, S. Bellemin-Laponnaz, L. H. Gade, *Chem. Soc. Rev.* **2004**, 619–636.

[7] J.-M. Suisse, S. Bellemin-Laponnaz, L. Douce, A. Maisse-François, R. Welter, *Tetrahedron Lett.* **2005**, *46*, 4303–4305.

[8] R. C. Weast, *Handbook of Chemistry and Physics*, 64th ed., CRC Press, Cleveland, **1983**.

[9] a) P. Seurin, D. Guillon, A. Skoulios, *Mol. Cryst. Liq. Cryst.* **1981**, *71*, 51; b) L. Douce, R. Ziessel, R. Seghrouchni, A. Skoulios, E. Campillo, R. Deschenaux, *Liq. Cryst.* **1996**, *20*, 235–242.

[10] F. Glorius, G. Altenhoff, R. Goddard, C. Lehmann, *Chem. Commun.* **2002**, 2704–2705.

[11] M. Poyatos, A. Maisse-François, S. Bellemin-Laponnaz, L. H. Gade, *Organometallics* **2006**, *25*, 2634–2641.

[12] PLATON, A Multipurpose Crystallographic Tool, A. L. Spek, *J. Appl. Crystallogr.* **2003**, *36*, 7–13.

[13] R. G. Pearson, *Inorg. Chem.* **1973**, *12*, 712–713.

[14] For a review of metal-catalyzed cross-coupling reactions, see: F. Diederich, P. J. Stang (Eds.), *Metal-Catalyzed Cross-Coupling Reactions*, Wiley-VCH, New York, **1998**; J. Dupont, R. F. de Souza, P. A. Z. Suarez, *Chem. Rev.* **2002**, *102*, 3667–3692; J.-C. Xiao, B. Twamley, J. M. Shreeve, *Org. Lett.* **2004**, *6*, 3845–3847.

[15] G. A. Grasa, M. S. Viciu, J. Huang, C. Zhang, M. L. Trudell, S. P. Nolan, *Organometallics* **2002**, *21*, 2866–2873.

[16] K. Okamoto, S. Nakajima, A. Itaya, S. Kusabayashi, *Bull. Chem. Soc. Jpn.* **1983**, *56*, 3830–3832.

[17] H. Tokuhisa, M. Era, T. Tsutsui, *Adv. Mater.* **1998**, *10*, 404–406.

[18] M. Funahashi, J. Hanna, *Appl. Phys. Lett.* **1997**, *71*, 602–604.

[19] M. Funahashi, J. Hanna, *Phys. Rev. Lett.* **1997**, *78*, 2184–2187.

[20] G. M. Sheldrick, *SHELXL97*, University of Göttingen, Germany, **1997**.

Received: February 27, 2007